





## Baseflow Characteristics in Alpine Rivers - a Multi-catchment Analysis in Northwest China

**GAN Rong**<sup>1,2</sup>  <http://orcid.org/0000-0002-5534-2986>; e-mail: ganrong168@163.com

**SUN Lin**<sup>1</sup>  <http://orcid.org/0000-0002-9730-5534>; e-mail: sunlin-cas@hotmail.com

**LUO Yi**<sup>1</sup>  <http://orcid.org/0000-0002-7245-3004>;  e-mail: luoyi@igsnr.ac.cn

*1 Key Laboratory of Ecosystem Network Observation and Modeling, Institute of Geographic Sciences and Natural Resources Research, Chinese Academy of Sciences, Beijing 100101, China*

*2 University of Chinese Academy of Sciences, Beijing 100049, China*

**Citation:** Gan R, Sun L, Luo Y (2015) Baseflow characteristics in alpine rivers - A multi-catchment analysis in Northwest China. *Journal of Mountain Science* 12(3). DOI: 10.1007/s11629-013-2959-z

© Science Press and Institute of Mountain Hazards and Environment, CAS and Springer-Verlag Berlin Heidelberg 2015

**Abstract:** As a component of streamflow, baseflow is critical for regulating seasonal distribution of river flows and stabilizing water supplies. Water resources in the arid area of Northwest China are mainly from multiple catchments in the alpine that could be influenced by varieties of climatic, land cover, soil and geological factors. While numerous studies have been done on streamflow, systematic analysis of baseflow in the alpine river systems is scarce. Based on historical daily streamflow data and the automated digital filter method of baseflow separation, this study investigated characteristics of hydrographs of overland flow, streamflow and baseflow of river systems fed by rainfall, snowmelt, glacier melt or mixtures of these. This study also calculated the recession constants and baseflow indices of 65 river systems. While the recession constant was 0.0034–0.0728 with a mean of 0.018, the baseflow index was 0.27–0.79 with a mean of 0.57. Further, Spearman's correlation analysis showed that the baseflow index was significantly correlated with catchment climatic factors (e.g., precipitation and temperature), topographic factors (e.g., elevation and slope) and aquifer properties represented by the recession constant. Multiple regression analysis indicated that the factors explained 65% of the variability of baseflow index in the study area.

**Received:** 6 May 2014  
**Accepted:** 15 August 2014

**Keywords:** Baseflow index; Recession constant; Snowmelt; Glacier melt; Streamflow

### Introduction

The total runoff hydrograph is the sum of surface runoff and baseflow (Nathan and McMahon 1990; Viessman and Lewis 2002). Baseflow is an important part of streamflow that is largely stable. A better understanding of baseflow could enhance the estimation of small-to-medium water supplies and the development of water management strategies, especially for drought conditions (Mwakalila et al. 2002). In addition, baseflow maintains the flow necessary for navigation, water supply, hydroelectric power and recreational uses in reservoirs (Santhi et al. 2008). Such an understanding could also be used to calibrate and/or validate hydrological models (Eckhardt 2008). Watershed planners determine water availability, water allocations, stream assimilation capacity and aquatic habitat needs by estimating the contributions of baseflow to streams (Stuckey 2006).

Baseflow could comprise a number of

components that vary seasonally with different recession constants (Nathan and McMhon 1990). Baseflow is influenced by subsurface properties and hydrological processes above and below the land surface. In the alpine headwater catchments, snow and glacier melts are important contributors to streamflow. Using water-balance computation, Mark and Seltzer (2003) noted that glacier melt contributes 35% to streamflow in Yanamarey and Uruashraju catchments of Cordillera Blanca. Compiled published data suggest that glacier melt contributes to the total runoff in the range of 0.1%–86% for 64 rivers in Northwest China (Yang 1991). Snow and glacier can store precipitation as solid water and release it as liquid water later in the following seasons or years, which could alter hydrographs of rivers. Understanding baseflow features influenced by snow and glacier melt is important for water use planning and hydrological disaster preparedness of downstream water users.

Baseflow volume is another important element of streamflow. Baseflow index (BFI), calculated as the long-term ratio of baseflow to total streamflow (Institute of Hydrology 1980), is useful for analyzing baseflow characteristics (Abebe and Foerch 2006). Several studies have related baseflow to climatic and topographic factors, land cover and soil types, and hydrogeological properties, the impacts of which vary from catchment to catchment (Vogel and Kroll 1990; Ponce and Shetty 1995a, b; Nathan et al. 1996; Lacey and Grayson 1998; Haberlandt et al. 2001; Mwakalila et al. 2002; Longobardi and Villani 2008).

Some studies have used different lithologies to describe catchment geology (Lacey and Grayson 1998; Mazvimavi et al. 2005). For instance, Haberlandt et al. (2001) used effective porosity and saturated hydraulic conductivity to determine the effects of catchment geology on baseflow. However, other studies have achieved limited success using multivariate regression models to estimate baseflow from lithological properties. Vogel and Kroll (1992) showed that baseflow is highly correlated with the baseflow recession constant. The recession constant is defined as a parameter of the baseflow recession curve expressed by an exponential function (Hall 1968; Singh and Stall 1971) and can be easily obtained through the daily streamflow records at the recession stage. This

constant reflects the response of baseflow to changes in recharge and is considered to be a comprehensive index of hydro-geological complexity. It thus provides an alternative analysis of the effects of complicated hydrogeological properties of the aquifer system on baseflow. This can be used where lithological properties are not readily available, such as for most catchments in the alpine.

The livelihood of the people and economy of arid Northwest China rely heavily on water originating from the alpine headwater regions in the Altay, Tianshan, Kunlun and Qilian Mountain systems. The headwater regions are diverse in attributes such as area, elevation, aspect, land cover, aquifer property and climate. Due to their unique roles in the hydrological cycle, runoff generation and sensitivity to climate change, studies in the last decades have particularly focused on snow and glacier systems of the headwater regions. Due to climate change and the increasingly crucial role of baseflow in maintaining streamflow, especially in low flow periods, there is a growing interest in baseflow characteristics of snow/glacier-fed catchments. Better understanding of baseflow characteristics and their relation to the climatic, topographic, and geologic factors through analysis of multi-catchments with diverse features is not only a locally important issue in the arid area of the northwest China, but also of significant interest in the scientific community.

The objectives of this study were to (1) identify the unique features of the hydrographs of typical headwater catchments in Northwest China and (2) investigate the recession properties, baseflow index and baseflow factors of multi-catchment headwater regions in the arid region of Northwest China.

## 1 Materials and Methods

### 1.1 Catchment and streamflow data

The study investigated baseflow characteristics in 65 inland rivers covering an area of 2.27 million km<sup>2</sup> in arid region of Northwest China. This area includes the whole of Xinjiang province and parts of Gansu, Inner Mongolia, Qinghai and Ningxia provinces (Figure 1). The inland rivers originate from the mountains, flow through foothill oasis

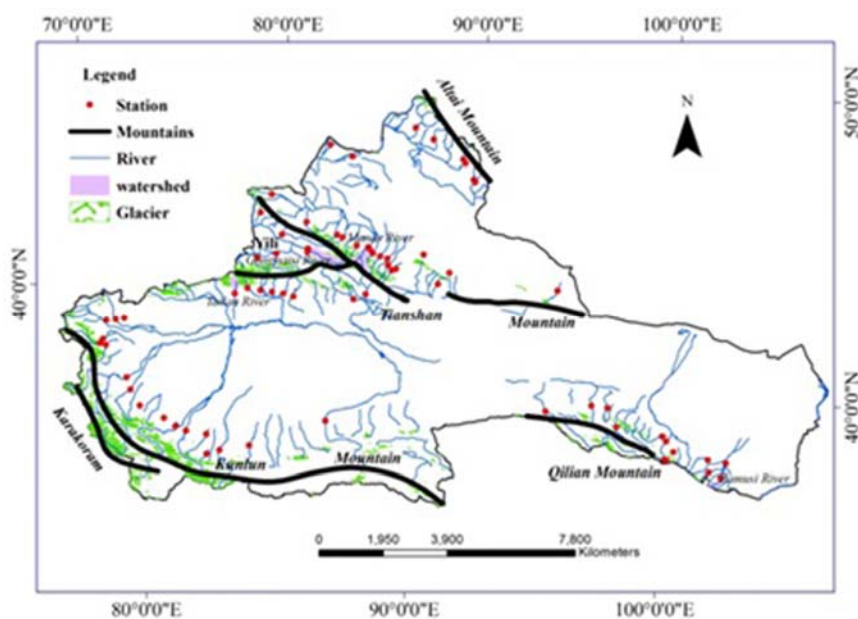


**Figure 1** Map of rivers and locations of runoff gauges in benchmark catchments in study area.

and end in deserts or desert lakes. There are actually over 500 rivers in the region, but only large rivers have routine streamflow monitoring gauges. The gauges are usually located at the outlets of the catchment from where the rivers flow out from the mountain ranges. The archives of monitoring data are usually inaccessible to the public, especially data collected after the 1990s. Officially released archives consisting of historical daily streamflow records for 65 gauges were used in the study. The time span of the gauge records was 7–36 years, with a mean of 23 years. The range of annual volume of streamflow for the 65 gauged rivers was  $0.29 \times 10^8$ – $64.33 \times 10^8$  m<sup>3</sup>. With streamflow measuring stations at river outlets, the boundaries of the benchmark catchments were derived from a digital elevation model (DEM) with grid size of 90 m × 90 m (CGIAR-CSI). The DEM was also used to derive various topographic attributes of the catchment, e.g., catchment area, average slope and elevation (Table 1).

Precipitation and temperature data were used to analyze baseflow characteristics of the rivers.

**Table 1 Basic features of the 65 benchmark catchments used in the study**

Variables	Min	Max	Mean	Std dev
Area (km <sup>2</sup> )	241	52152	5614	8290
Elevation (m)	1785	4935	3139	735
Slope (°)	8	30.5	21.4	5.3

Observed precipitation data are scarce in the alpine catchments. Of the 65 catchments, precipitation and temperature data are officially released by China’s Ministry of Meteorology for only 38 catchments.

The ratio of glacier melt contribution to streamflow was defined as the melt water of snow and ice in the glacierized area to total runoff. The contribution ratios of glacier melt water to streamflow in arid Northwest China have long been of interest to glaciologists and hydrologists (Kang 1983; Yang 1991; Gao et al. 2010). Snowmelt and rainfall runoff

are other two important sources of streamflow in arid Northwest China. The contributions of glacier, snow and rainfall components to total streamflow vary significantly from river to river. Thus Yang (1980) grouped the rivers into four categories based on the sources of recharge—glacier melt water recharge, seasonal snowmelt water recharge, rainfall recharge and snow/glacier melt water recharge. Out of the 65 benchmark catchments, four typical catchments were selected to study the characteristics of baseflow hydrographs of the four river systems grouped on the basis of recharge source (Table 2).

### 1.2 Baseflow separation

Among the commonly used techniques for separating baseflow from streamflow are graphical methods (Arnold 1995; Dong and Deng 2005) and digital filters (Nathan and McMahon 1990). Because graphical separations are highly subjective and time consuming (Hewlett and Hibbert 1967; Anderson and Burt 1980), the simpler digital filters are more widely used (Nathan and McMahon 1990; Arnold and Allen 1999; Arnold et al. 2000; Szilagyi 2004; Eckhardt 2005, 2008; Santhi and Allen 2008; Longobardi and Villani 2008). Applications of digital filters suggest that the method yields a

more realistic and stable estimate of baseflow or BFI (Nathan and McMahon 1990; Santhi and Allen 2008).

Originally, the digital filter method was used in signal analysis and processing (Lyne and Hollick 1979). Filtering surface runoff (high frequency signals) from baseflow (low flow signals) is similar to filtering high frequency signals in signal processing. The digital filter equation is given by Nathan and McMahon (1990) as:

$$q_t = \beta q_{t-1} + (1 + \beta) / 2 \times (Q_t - Q_{t-1}) \tag{1}$$

where  $q_t$  is filtered surface runoff at time step  $t$ ,  $Q_t$  is streamflow and  $\beta$  is filter parameter for attenuation. Then baseflow volume  $b_t$  is calculated as:

$$b_t = Q_t - q_t \tag{2}$$

The value of the filter parameter that yields the most acceptable baseflow separation is in the range of 0.9–0.95, the optimal value being 0.925. As suggested by Nathan and McMahon (1990), and more widely used in baseflow analysis (Fan et al. 2014, Aksoy et al. 2009, Partington et al. 2012, Fan et al. 2013), the filter parameter in this study was set at 0.925. An automated digital filter (Arnold et al. 1995) can pass over streamflow data three times – forward, backward and forward. Passing the filter through streamflow data multiple times systematically lowers percent baseflow. Thus an automatic baseflow filter program was used in this study to separate baseflow and calculate baseflow recession constant from daily streamflow records.

The Spearman’s correlation analysis was used to determine the correlation coefficients between BFI and topographic, climatic and geologic parameters in the catchments. Then statistical linear regression models were used to quantify factor controls on BFI as in Santhi and Allen (2008), Bloomfield et al. (2009) and Zhu and Day (2009).

### 1.3 Baseflow recession constant

Several studies have demonstrated that baseflow recession curve can be fitted to exponential decay function (Hall 1968; Singh and Stall 1971) as follows:

$$Q_t = Q_0 \cdot \exp(-\alpha t) \tag{3}$$

where  $Q_t$  is streamflow at time  $t$ ,  $Q_0$  is initial streamflow at start of recession, and  $\alpha$  is baseflow recession constant. The exponential function implies that the aquifer reacts like a single linear reservoir where storage is proportional to outflow. The recession constant is determined by rearranging Eq. (3) as follows:

$$\alpha = \frac{1}{N} \ln \frac{Q_N}{Q_0} \tag{4}$$

where  $N$  is the number of days from start of recession. Baseflow days is the number of days for baseflow recession to decline through one log cycle. Baseflow days are commonly reported for watersheds. Thus Eq. (4) can further be simplified as follows:

$$\alpha = \frac{1}{BFD} \ln(10) \tag{5}$$

where  $BFD$  is number of baseflow days for the watershed.

The baseflow recession constant “ $\alpha$ ” is a direct index of groundwater flow response to changes in recharge. It is a highly useful parameter in describing baseflow and catchment features. Large  $\alpha$  value signifies a steep recession which is indicative of rapid drainage and little storage. Small  $\alpha$  value implies a long delay of baseflow and a slow release of groundwater in a catchment (Vogel and Kroll 1992). In this study,  $\alpha$  values of the selected catchments were derived using Eq. (5) and daily streamflow records during the low flow period. Baseflow recession constant was used as a

**Table 2 The main characteristics of the four typical catchments of the four river systems grouped on the basis of recharge source in the arid of Northwest China**

River type	River name	Catchment area (km <sup>2</sup> )	Ave.elevation (km <sup>2</sup> )	Glacier area ratio (%)	Annual flow (10 <sup>8</sup> m <sup>3</sup> )	Glacier melt contribution (%)
Glacier-fed	Tailan	1498	3734	45.9	7.27	74
Glacier-snow-fed	Manas	5027	3304	14.3	11.7	34.6
Snow-melt	Gongnaisi	4123	2134	1.3	14.6	2
rainfall-fed	Zamusi	846	3488	0.7	2.36	1.4

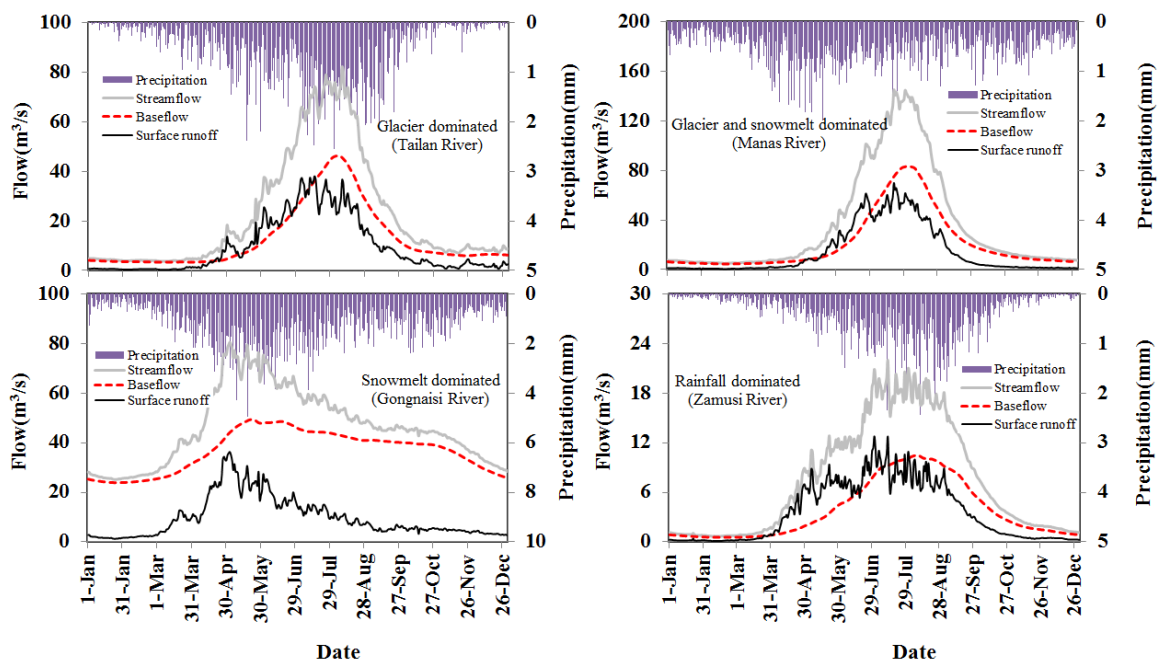


**Figure 2** Hydrographs of streamflow, overland flow and baseflow for four rivers of different river systems (grouped by recharge sources) in the arid of Northwest China.

proxy index to describe catchment geology and to discuss the relationship between baseflow and catchment aquifer properties.

## 2 Results and Discussions

### 2.1 Hydrographs for typical catchments

#### 2.1.1 Overland flow and streamflow

Hydrographs of streamflow, overland flow and baseflow for the four typical catchments of different recharge types are depicted in Figure 2. Hydrographs of all the four river systems are apparently influenced by seasonal distribution of precipitation. Rain is a dominant factor of runoff in rain-fed Zamusi River — which is located in the Qilian Mountains with low elevation, generally higher temperatures and less frequent snowfall than in the other catchments. Glacier melt contribution to streamflow was as low as 1%. The rise and fall of the hydrograph for the overland flow coincided with seasonal distribution patterns of precipitation. Due to baseflow regulation, a time lag was noted in high flow periods for streamflow (as discussed further in the next sections). The quick response of runoff to rainfall was a vital feature of this river type.

Snowmelt stored in winter was released in spring, causing high flows in spring and early summer — as depicted in the hydrograph for snow-fed Gongnaisi River in Figure 2. Gongnaisi River is a major tributary of Ili River and is located in the upper reach of the river. The Ili valley, which is like a trumpet facing the westerlies, receives relatively high precipitation compared with other regions of the arid Northwest China. The valley also has a colder temperature in winter with frequent snowfall in late autumn through early spring. Sometimes heavily snowstorms occur in the valley, causing severe disasters for both human and livestock. This implies that huge amounts of precipitation are stored during the cold season. Figure 3 depicts the distribution of snow pack derived from MODIS (Moderate Resolution Imaging Spectroradiometer) data. The snow melts in warmer temperatures in late spring and releases stored water into the rivers, sometimes rapid enough to cause flash floods. In Figure 2, a sharp rise in the hydrographs of surface runoff and streamflow was characteristic of Gongnaisi River dominated by snowmelt.

The hydrographs were dominantly driven by glacier melt in catchments with less snowmelt and rainfall runoff. This was the case for Tailan River, where glacier melt contributed as much as 74% of

streamflow. The Tailan River is in the southern slope of Tianshan Mountains, with relatively high elevation and a high glacier area coverage ratio. Snowfall is high in high elevation zones and low in low elevation zones of the catchment. Snow and glacier melt dominate surface runoff and streamflow hydrographs (Figure 2). With temperature rises in spring through autumn and from the lower to upper zones of the catchment and along with less cloud cover, solar radiation energy increases (Meier, 1969), glacier melt develops, hits peak value in August and then recedes in mid-October as temperatures drop below the melting point. The instant response of glacier melt to a sudden rise in temperature could cause flash floods and outbursts of glacier lakes (Sheng et al. 2009), risking potential damages to downstream water users.

Glaciers are fed by snow and discharged by the effects of temperature and wind, regulating intra/inter-annual precipitation-runoff processes in the catchments. It has been noted that continental glaciers delay precipitation-runoff transformation by tens or even hundreds of years due to the slow turnover rate of snow to ice and dynamic movement of ice from accumulation areas to ablation zones (Xie and Liu 2010). Thus the long-term effect of glacier melt on the hydrographs is usually investigated by hydrological simulation over hundreds of years (Qing 2006; Immerzeel et al 2013). This is currently the trend of research on the impacts of climate change on glacier/snow-dominated watershed hydrology (Unger-Shayesteh et al. 2013). The interactive effects of precipitation, glacier and temperature determine the shapes of the hydrographs. In catchments where rainfall, snow and glaciers equally contribute to runoff generation, overland flow and streamflow hydrographs followed a steady rise and fall; as noted for Manas River catchment in Figure 2. The Manas River is located in the northern slope of the Tianshan Mountains, which is cold in late winter through spring and warm in summer through autumn. While the precipitation is mainly concentrated in summer, a large amount of the precipitation falls as snow in late autumn through

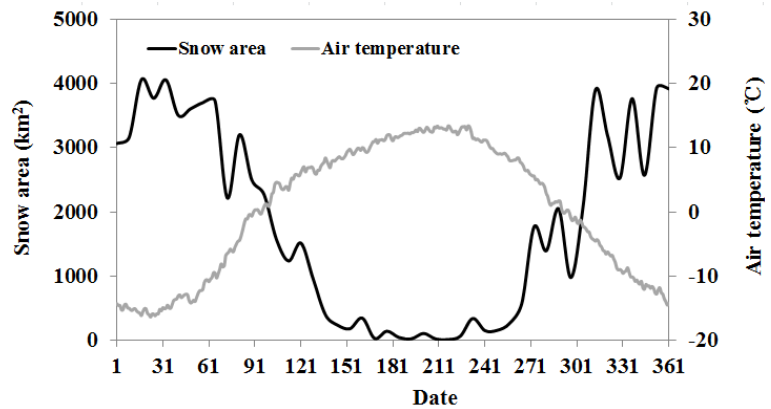


**Figure 3** Seasonal changes in snow area as estimated from MODIS and air temperature data in Gongnaisi River catchment in the arid region of Northwest China.

winter. This is especially common in high elevation zones of the catchment. Glacier area covers approximate 718 km<sup>2</sup>, accounting for some 14.3% of the catchment area (Table 2). Estimates by different studies suggest that glacier melt accounts for some 30% of the total runoff (Yang 1991; Tang et al. 2011). The contributions of rainfall and snowmelt runoff to streamflow were similar. Low temperatures and sufficient precipitation induced high water storage in winter. Then rising temperatures in spring triggered release of the stored water. Snow water release slowed down or even sopped in late spring, followed by glacier melt in high elevation zones and rainfall runoff in medium and low elevation zones. The overland flow and streamflow increased steadily until peak value in mid to late July. Glacier melt was a key contributor to streamflow until late September and diminished to almost insignificant level in early October as temperatures dropped below melting point in glacier zones. Snow, rainfall and glaciers sequentially dominated to runoff generation under the interactive effects of precipitation and temperature and their combined distributions along seasonal, horizontal and altitudinal gradients.

### 2.1.2 Baseflow hydrographs

The baseflow hydrographs were influenced by aquifer recharge, aquifer storage and storage release. From the illustration in Figure 2, the baseflow hydrographs followed the rising and falling of the overland flow with some delays in the phases. The point of onset of baseflow in the rising phase was earlier in rivers fed by rainfall and

**Table 3 Baseflow features of different river types in the arid region of Northwest China**

River type	River name	Spr.-B(%)	Sum.-B (%)	Aut.-B (%)	Win.-B(%)	MCV	ACV
Glacier-fed	Tailan	10	62	21	8	0.97	0.12
Glacier-snow-fed	Manas	8	64	20	7	1.05	0.09
Snow-fed	Gongnaisi	25	31	26	18	0.22	0.25
Rainfall-fed	Zamusi	11	55	29	5	0.88	0.33

**Notes:** Spr.-B = Spring baseflow (March to May); Sum.-B = Summer baseflow (June to August); Aut.-B = Autumn baseflow (September to November); Win.-B= Winter baseflow (December to February); MCV = Monthly coefficient of variation; ACV = Annual coefficient of variation

snowmelt than that in rivers fed by glaciers. In fact, baseflow primarily originated from infiltration of liquid water from the surface into the soil profiles and deep percolation to the aquifer systems. The infiltration properties of the soil profiles and distance to the aquifer determined the rate and volume of water percolation to the aquifer systems. For the alpine catchments, soil profile temperature is usually low and soils may freeze within few meters below land surfaces-whether or not they are covered by snow (Wu et al. 2007; Cheng et al. 2007). In early spring, soil infiltration capacity could significantly reduce and in turn hinder infiltration of water from rain or snowmelt (Guo et al. 2005; Wang 2013). The aquifer becomes depleted in the winter because of insufficient recharge from the soil profile. The delayed response was reasonable, given the effects of watershed surface storage, retention and soil freezing/thawing on infiltration and recharge (Luo et al. 2012; Gan and Luo 2013). Baseflow shifted the peaks of streamflow hydrographs to the right. The delay of baseflow in relation to overland flow was best expressed by the recession constant in Eq. (4). Smaller recession constants implied longer delays and vice versa. Of the four river types, Gongnaisi River had the longest delay time as given by the smallest recession constant. Then the recession constants for Manas and Tailan Rivers were similar and that for Zamusi River was the largest, implying the shortest baseflow delay time. Flatter baseflow hydrographs with smaller recession constants suggested stronger stabilizing effects of the aquifer systems in the catchments on seasonal streamflow. This is important for a sustained water supply to downstream users and mitigates both flood and drought disasters. This is especially important for rivers without facilities for streamflow regulation and storage. Because data on hydrogeological properties of aquifer systems in

alpine catchments are not readily available, the recession constant can effectively reflect aquifer properties. This is especially applicable to aquifer transmissivity and storage (Ford and Williams 1989; Eckhardt 2008; Santhi and Allen 2008), which are useful in streamflow management.

Baseflow volume varied significantly both intra-annually and inter-annually. For all the four typical catchments, baseflow in June through August was highest, generally accounting for over half of the annual total (Table 3). Baseflow in winter was very small, with a portion mostly less than 10%. The monthly coefficients of variation in baseflow for rain/snow-fed rivers were less than that of glacier-fed rivers. Contrary to the variation at the monthly scale, annual coefficients of variation for glacier-fed rivers were much smaller than those of rain/snow-fed rivers. A similar trend was reported for the rivers in the North Cascade Mountains of Washington State (Fountain and Tangborn 1985). Glaciers are frozen reservoirs of water that could regulate annual flow fluctuations by storing water in cool/wet conditions and providing water in warm/dry periods. This not only compensates for water supply in dry years, but also provides a drought buffer (Chennault 2002).

## 2.2 Multi-catchment baseflow analysis

### 2.2.1 Baseflow recession constants

Baseflow recession constants calculated using the digital filter and historical streamflow records for 65 benchmark catchments are listed in Table 4. Statistical analysis showed that although the constants varied significantly for the 65 benchmark catchments, they followed a normal distribution with a mean value of 0.018. The constants were randomly distributed in space with no clear spatial pattern (Figure 4). Catchments with recession constants larger than 0.04 include Duwa river,

Cherchen river and Liyuanbao River basins; originating from Karakoram, Kunlun and Qilian Mountains, respectively. The large recession constants represented quick response and short durations of baseflow. The estimated average baseflow days of the rivers were respectively 32 d, 43 d and 50 d. Quick response of baseflow to recharge and release could trigger sharp rising and falling phases of streamflow hydrographs. On the one hand, flash floods could occur and cause potential damages to engineering facilities and downstream water users. On the other hand, uneven seasonal distribution of streamflow does not support a sustainable water supply for downstream water users. For instance, the Cherchen River has a catchment area of over 30 000 km<sup>2</sup> and annual streamflow of 5.0 × 10<sup>2</sup> m<sup>3</sup>, and is the sole source of water for Qiemo County. It is ranked as the second largest catchment in China

(in terms of area) and over 60,000 people live in the downstream region of the river. Under extreme dry climate conditions, fragile riparian ecosystems in the downstream region of the river also heavily rely on the water. The relatively large recession constant suggested that for more efficient water resources use, it is important to construct streamflow regulation facilities on Cherchen River.

### 2.2.2 Baseflow index

BFI, defined as the ratio of baseflow volume to streamflow volume, varied significantly in the range of 0.27–0.79 (Table 4). As graphically depicted in Figure 5, BFI for rivers originating from the Qilan Mountains, the Tianshan Mountains and the Eastern Pamir exceeded 0.5 and sometimes 0.7. Then BFI for rivers originating from the Karakoram and Kunlun Mountains was less than 0.5 and sometimes less than 0.3. Catchments with

**Table 4 Baseflow index (BFI) and baseflow recession constant (α) for 65 benchmark catchments in the arid area of Northwest China**

River	Hydro-station	Area (km <sup>2</sup> )	BFI	α	River name	Hydro-station	Area (km <sup>2</sup> )	BFI	α
Buerjin	Qunkule	9218	0.59	0.0181	Kashi	Tuohai	10296	0.68	0.0046
Kelan	Alaer	1638	0.47	0.0123	Kukesu	Kukesu	5872	0.60	0.0114
Kayiertes	Kuwei	2427	0.52	0.0186	Aheyaz	Aheyaz	2887	0.57	0.0111
Kuyiertes	Fuwun	2019	0.49	0.0197	Qiedek	Qiedek	322	0.65	0.0095
Qinggil	Dig Qinghe	1678	0.45	0.0323	Boertal	Wenquan	2461	0.66	0.0055
Ulungur	Small Qinghe	1344	0.47	0.0234	Jinghe	Jingheshank	1515	0.6	0.0149
Kalayiml	Kalayiml	314	0.5	0.0261	Sikesu	Jiele	978	0.56	0.0223
Kalanggue	Kalanggue	3739	0.58	0.0191	Kuntun	Jialeguol	1957	0.64	0.0143
Gongnaisi	Ceketai	4403	0.79	0.0096	Jinggou	Bajiahu	1462	0.56	0.0182
Qiafu	Qiafu	1517	0.72	0.0105	Manas	Kensiwate	5027	0.61	0.0151
Qingshuihe	Qingshuihe	450	0.61	0.0174	Huangshuigou	Huangshuigou	4553	0.57	0.0186
Taxi	Shimenz	622	0.62	0.0169	Kandu	Dashankou	19261	0.75	0.0083
Hutub	Shimen	1912	0.6	0.0159	Kuche	Langan	3174	0.52	0.0176
Santun	Zhanpanz	1806	0.6	0.0304	Kalas	Kalas	1430	0.46	0.0208
Toutun	Zhicaichang	891	0.59	0.0185	Heizi	Heizi	3342	0.6	0.0102
Urumqi	Yingxiongqiao	969	0.56	0.0175	Kamusil	Kamuluk	2019	0.54	0.0115
Muzhati	Ahebulong	3090	0.54	0.0117	Tailan	Tailan	1498	0.58	0.0142
Meiyaogou	Meiyaogou	512	0.53	0.0125	Qiakemak	Qiaqig	4308	0.57	0.0120
Kaiken	Kaiken	396	0.53	0.0166	Kalangguluk	Kalangguluk	2080	0.55	0.0156
Weizixia	Weizixia	1149	0.76	0.0034	Buguz	Ae river	2498	0.68	0.0093
Weitak	Weitak	600	0.54	0.0111	Kushan	Shaman	2474	0.55	0.0140
Yerqiang	Kaqun	52152	0.55	0.0113	Gaizi	Kelek	10466	0.59	0.0134
Tizinafu	Yuzimlek	6286	0.42	0.0181	Dang	Dangchengw	19522	0.76	0.0144
Pishan	Pishan	2202	0.43	0.0171	Changma	Changmabao	11034	0.56	0.0218
Duwa	Duwa	866	0.46	0.0728	Heihe	Yingluoxia	10006	0.60	0.0165
Cherchen	Qiemo	32077	0.29	0.0537	Taolai	Zhulongguan	5336	0.76	0.0063
Kalakashi	Wuluwat	22433	0.44	0.0194	Heihe	Zhamashenk	5025	0.60	0.0323
Yulongkashi	Tongguziluok	15786	0.44	0.0143	Dazhum	Wafangc	241	0.51	0.0161
Nuer	Nuer	1012	0.27	0.0164	Zamu	Zamus	846	0.53	0.0196
Keliya	Nunmaitig	15833	0.49	0.0128	Xiyiing	Jiutiaoling	1084	0.51	0.0174
Heihe	Qilian	2456	0.53	0.0246	Liyuan	Liyuanbao	2386	0.44	0.0457
Hongshui	Hongshuih	3286	0.77	0.0140	Haba	Kelatashen	6111	0.59	0.018
Piliqin	Piliqin	794	0.67	0.0108					



BFI greater than 0.5 accounted for 77% and those with BFI greater than 0.7 accounted for only 11% of the 65 investigated benchmark catchments. Averaged BFI for the catchment river systems was 0.57. This suggested that baseflow was a significant portion of streamflow in arid regions of Northwest China, further implying that baseflow was critical for stabilizing seasonal distributions of streamflow in the study area.

Statistical parameters of correlation analysis between BFI and selected potential factors of baseflow are summarized in Table 5. At P (significance level) of less than 0.05, the correlation is considered to be significant.

BFI was significantly correlated with catchment precipitation and hydro-geological properties. Spearman's correlation coefficient suggested that the higher the precipitation, the larger the baseflow component. It also suggested that BFI had a significant negative correlation with recession constant. It was assumed that more precipitation as either snow or rain generated more aquifer recharge. Lacey and Grayson (1998) noted a similar phenomenon for a river in Victoria, Australia. However, Haberlandt et al. (2001) noted a negative correlation for the Elbe River Basin in Germany with a mean annual rainfall 700 mm, much more than the rivers investigated in this study. The negative correlation in Elbe River Basin could be due to runoff generation under saturated storage conditions. Under these conditions, abundant rainfall induces high soil moisture content and dominant surface runoff.

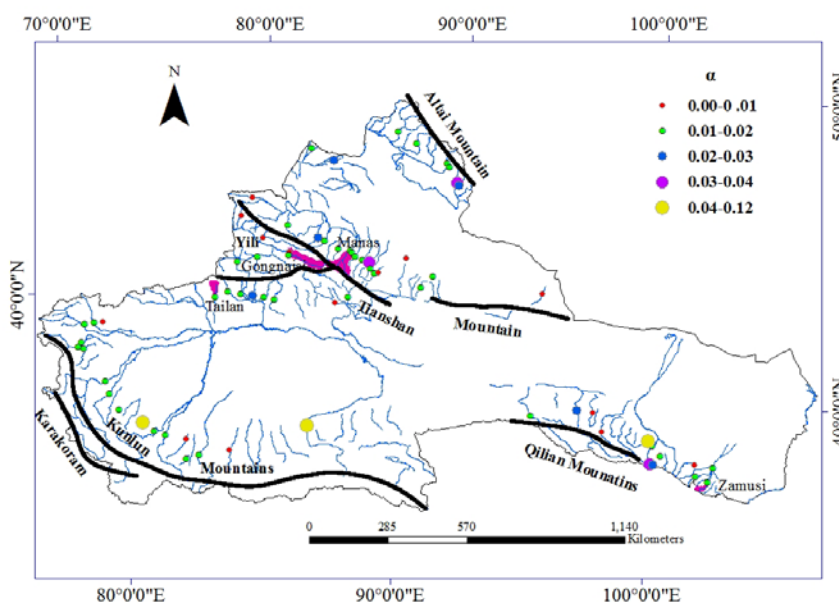


**Figure 4** Distribution map of recession constants for 65 benchmark catchments in the arid area of Northwest China.

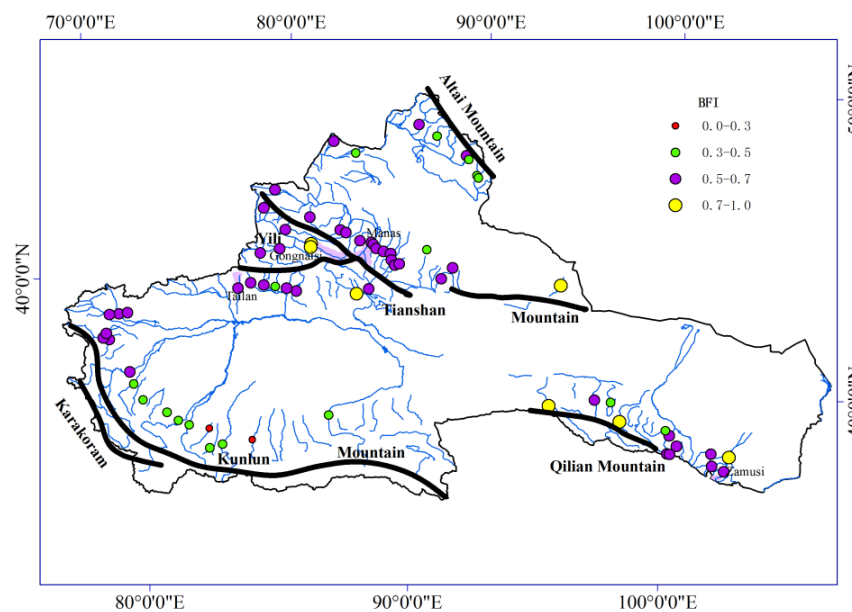


**Figure 5** Distribution map of baseflow indices for 65 benchmark river systems in arid area of Northwest China.

A negative correlation ( $-0.56, P < 0.01$ ) was observed between BFI and baseflow recession constant in the study area. Infiltration and storage capacities in catchments with larger recession constant were lower, implying rapid drainage. This condition is not good for groundwater recharge and storage in the study area. Snow/glacier melt or rainfall contributed to river flow via surface runoff, resulting in a small BFI for the catchments.

A significant negative correlation was noted between BFI and topographic factors such as elevation and slope. Steeper slopes induced stronger overland flows and weaker infiltration rates. For higher altitude catchments, the largely frozen soils due to negative autumn, winter and spring temperatures (Figure 6) limited snow/glacier melt water infiltration. A negative correlation was also observed between BFI and air temperature. Thus the effect of air temperature on BFI could be similar to that of elevation on BFI as air temperature decreases with increasing altitude.

Multi-regression analysis was conducted to further investigate the overall correlation between the BFI and climatic factors, topographic factors and aquifer parameters. Based on the multi-regression analysis, the overall coefficient of determination for the tested variables was 0.65. This suggested that climatic factors such as precipitation and temperature, topographic factors such as elevation and slope, and aquifer parameters such as recession constant together explained only 65% of the variability of BFI in the study area. This implied that some other factors influenced the characteristics of rivers/catchments (e.g., baseflow and streamflow) in arid area of Northwest China. It should be noted that the average values of the climatic and topographic factors for the catchments and the lumped recession constant for the properties of the aquifer systems in the catchments could have degraded the BFI signal.

### 3 Conclusions

This paper analyzed the features of baseflow

**Table 5 Summary of the Spearman's correlation analysis for baseflow index and physical properties of 65 investigated benchmark catchments in arid area of Northwest China**

Variables	Precipitation	Temperature	Mean elevation	Mean slope	Recession constant
Rs	0.60	-0.33	-0.33	-0.34	-0.56
P	0.000	0.044	0.008	0.005	0.000
N	38	38	65	65	65

**Notes:** Rs = Spearman's correlation coefficient; P= significance level; N= number of samples

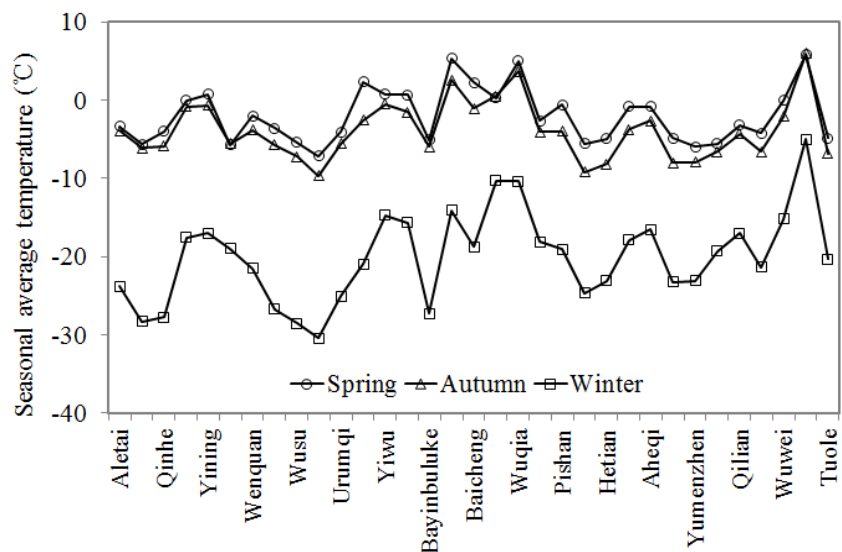


**Figure 6** Mean temperatures for autumn, winter and spring in the catchments of arid area of Northwest China.

hydrographs for four rivers of different recharge types (glacier-fed, glacier/snow-fed, snow-fed and rain-fed rivers) and the investigated recession constants and BFI of 65 benchmark catchments in arid area of Northwest China. The analysis used historical daily streamflow data and a digital filter method to separate baseflow.

The study showed that the range of recession constants in the study area was 0.0034–0.0728, with a mean of 0.018 and no spatial distribution pattern. The range of BFIs in the study area was 0.27–0.79, with a mean of 0.57. It suggested that the contribution of baseflow to streamflow was larger than that of overland flow in the arid area of Northwest China.

It was concluded that BFI was driven by a group of factors. Spearman correlation analysis showed that BFI was correlated with precipitation ( $R^2 = 0.60$ ) and recession constant ( $R^2 = -0.56$ ) at  $p < 0.001$ . The negative correlation of BFI with

recession constant might be attributed to that the large recession constant may represent a slow transmissivity and slow release of the aquifer, which causes a low baseflow. It was also noted that the BFI was negatively correlated with average slope and average elevation of catchments ( $P < 0.01$ ). The negative correlation might be due to low hydraulic conductivity of frozen soils, which also limited recharge in the alpine catchment aquifer systems. The steep slopes also induced high overland flow and thus low aquifer recharge.

Overland flow hydrographs of rain-fed river systems quickly responded to rainfall, those of snow-fed rivers showed a quick flow rise in spring, while those of glacier-fed rivers showed a rapid flow gain and loss in June-August glacier melt

season. Baseflow hydrographs were driven by the combined effects of precipitation, aquifer properties and topographic factors, and the patterns are diversified for the inland rivers in arid area of Northwest China.

## Acknowledgements

The research was partially funded by the International Co-operation Program of the Ministry of Science and Technology of China (Grant No. 2010DFA92720), and the Project of the National Eleventh-Five Year Research Program of China (Grant No. 2012BAC19B07).

## References

- Abebe A, Foerd G (2006) Catchment characteristics as predictors of base flow index (BFI) in Wabishebele river basin, east Africa. Conference on International Agricultural Research for Development, Siegen, Germany, October 11-13, 2006.
- Aksoy H, Kurt I, Eris E (2009) Filtered smoothed minima baseflow separation method. *Journal of Hydrology* 372: 94-101. DOI:10.1016/j.jhydrol.2009.03.037
- Anderson MG, Burt TP (1980) Interpretation of recession flow. *Journal of Hydrology* 46: 89-101.
- Arnold JG, Allen PM (1999) Automated methods for estimating baseflow and ground water recharge from streamflow records. *Journal of the American Water Resources Association* 35: 411-424.
- Arnold JG, Allen PM, Muttiah R, et al. (1995) Automated base flow separation and recession analysis techniques. *Ground Water* 33: 1010-1018.
- Arnold JG, Muttiah RS, Srinivasan R, et al. (2000) Regional estimation of baseflow and groundwater recharge in the Upper Mississippi river basin. *Journal of Hydrology* 227: 21-40.
- Bloomfield JP, Allen DJ, Griffiths KJ (2009) Examining geological controls on baseflow index (BFI) using regression analysis: An illustration from the Thames Basin, UK. *Journal of Hydrology* 373: 164-176. DOI: 10.1016/j.jhydrol.2009.04.025
- Chen RS, Kang ES, Ji XB, et al. (2007) Preliminary study of the hydrological processes in the alpine meadow and permafrost regions at the headwaters of Heihe River. *Journal of Glaciology and Geocryology* 29: 387-396.
- Chennault JW (2002) Contributions of glacial meltwater to streamflow at Thunder Creek, using a distributed hydrology model, North Cascades National Park, Washington. Western Washington University, Washington, USA.
- Dong XG, Deng MJ (2005) Xinjiang groundwater resources. Xinjiang: Xinjiang Science and Technology Press. pp 88-92. (In Chinese)
- Duan JJ, Cao XL, Shen YP, et al. (2010) Surface water resources and its trends in Weigan River basin on the south slope of Tianshan, China during 1956-2007. *Journal of Glaciology and Geocryology* 32(6): 1211-1219. (In Chinese)
- Eckhardt K (2005) How to construct recursive digital filters for baseflow separation. *Hydrological Processes* 19: 507-515. DOI: 10.1002/hyp.5675
- Eckhardt K (2008) A comparison of baseflow indices, which were calculated with seven different baseflow separation methods. *Journal of Hydrology* 352: 168-173. DOI: 10.1016/j.jhydrol.2008.01.005
- Fan Y, Chen Y, Li W (2014) Increasing precipitation and baseflow in Aksu River since the 1950s. *Quaternary International* 336: 26-34.
- Fan Y, Chen Y, Liu Y, Li W (2013) Variation of baseflows in the headstreams of the Tarim River Basin during 1960-2007. *Journal of Hydrology* 487: 98-108.
- Ford D, Williams P (1989) Karst geomorphology and hydrology. Unwin Hyman Ltd., London 601.
- Fountain AG, Tangborn WV (1985) The effect of glaciers on streamflow variations. *Water Resource Research* 21 (4): 579-586.
- Gao X, Zhang SQ, Ye BS, et al. (2010) Glacier runoff change in the upper stream of Yarkant River and its impact on river runoff during 1961-2006. *Journal of Glaciology and Geocryology* 32(3): 445-453. DOI: 1000-0240(2010)03-0445-09 (In Chinese)
- Gan R, Luo Y (2013) Using the nonlinear aquifer storage-discharge relationship to simulate the baseflow of glacier- and snowmelt-dominated basins in northwest China. *Hydrology and Earth System Science* 17: 3577-3586. DOI: 10.5194/hess-17-3577-2013.
- Guo ZR, Han SP, Jing EC (2005) Recharge and loss of groundwater during freezing-thawing period in inland basin, Northwestern China. *Advances in Water Science* 26: 322-325.
- Hall FR (1968) Base flow recession, a review. *Water Resource Research* 4 (5): 973-983.
- Haberlandt U, Klocking B, Krysanova V, et al. (2001) Regionalisation of the base flow index from dynamically simulated flow components – a case study in the Elbe River Basin. *Journal of Hydrology* 248: 35-53.
- Hewlett JD, Hibbert AR (1967) Factors affecting the response of small watersheds to precipitation in humid areas. *Forest Hydrology*: 275-290.
- Immerzeel WW, Pellicciotti F, Bierkens MFP (2013) Rising river flows throughout the twenty-first century in two Himalayan

- glacierized watersheds. *Nature geoscience* 4: 742-745. DOI: 10.1038/NNGEO1896.
- Institute of Hydrology (1980) Low Flow Studies Report, Wallingford, UK.
- Kang ES (1983) Glacial meltwater runoff on the north flank of Bogda in Tianshan and its contribution to river flow. *Journal of Glaciology and Geocryology* 5: 114-122.
- Lacey CG, Grayson RB (1998) Relating baseflow to catchment properties in south-eastern Australia. *Journal of Hydrology* 204: 231-250.
- Longobardi A, Villani P (2008) Baseflow index regionalization analysis in a mediterranean area and data scarcity context: Role of the catchment permeability index. *Journal of Hydrology* 355: 63-75. DOI:10.1016/j.jhydrol.2008.03.011
- Luo Y, Arnold J, Allen P, Chen X (2012) Baseflow simulation using SWAT model in an inland river basin in Tianshan Mountain, Northwest China. *Hydrology and Earth System Sciences* 16: 1259-1267. DOI: 10.5194/hess-16-1259-2012.
- Lyne V and Hollick M (1979) Stochastic time variable rainfall runoff modeling. In: *Hydrology and Water Resources Symposium Perth 1979 Proceedings*. National Committee on Hydrology and Water Resources of the Institution of Engineers, Australia. pp 89-92.
- Mark BG, Seltzer GO (2003) Tropical glacier meltwater contribution to stream discharge: a case study in the Cordillera Blanca, Peru. *Journal of Glaciology* 49: 271-281.
- Mazvimavi D, Majerink AMJ, Savenije HHG, et al. (2005) Prediction of flow characteristics using multiple regression and neural networks: a case study in Zimbabwe. *Physics and Chemistry of the Earth* 30: 639-647. DOI: 10.1016/j.pce.2005.08.003.
- Mwakalila S, Feyen J, Wyseure G (2002) The influence of physical catchment properties on baseflow in semi-arid environments. *Journal of Arid Environments* 52: 245-258. DOI:10.1006/jare.2001.0947.
- Nathan RJ, Austin K, Crawford D, et al. (1996) The estimation of monthly yield in ungauged catchments using a lumped conceptual model. *Australian Journal of Water Resources* 1(2): 65-75.
- Nathan RJ, McMahon TA (1990) Evaluation of automated techniques for baseflow and recession analysis. *Water Resources Research* 26 (7): 1465-1473.
- Partington D, Brunner P, Simmons CT, et al. (2012) Evaluation of outputs from automated baseflow separation methods against simulated baseflow from a physically based, surface water-groundwater flowmodel. *Journal of Hydrology* 458-459: 28-39.
- Ponce VM, Shetty AV (1995a) A conceptual model of catchment water balance. 1. Formulation and calibration. *Journal of Hydrology* 173: 27-40.
- Ponce VM, Shetty AV (1995b) A conceptual model of catchment water balance. 2. Application to runoff and baseflow modeling. *Journal of Hydrology* 173: 41-50.
- Qing DH, Xiao CD, Ding YJ, et al (2006) Progress on cryospheric studies by international and Chinese communities and perspectives. *Journal of Applied Meteorological Science* 17 (6): 649-656.
- Santhi C, Allen PM (2008) Regional estimation of base flow for the conterminous United States by hydrologic landscape regions. *Journal of Hydrology* 351: 139-153. DOI: 10.1016/j.jhydrol.2007.12.018
- Sheng YP, Wang GY, Ding YJ, et al. (2009) Changes in Merzbacher lake of Inylchek glacier and glacial flash floods in Aksu River basin, Tianshan during the period of 1903-2009. *Journal of Glaciology and Geocryology* 31: 993-1001.
- Singh KP, Stahl JB (1971) Derivation of baseflow recession curves and parameters. *Water Resource Research* 7 (2): 292-303.
- Stuckey MH (2006) Low flow, base flow, and mean flow regression equations for Pennsylvania streams. US Geological Survey Scientific Investigations Report 2006-5130.
- Szilagyi J (2004) Heuristic continuous base flow separation. *Journal of Hydrological Engineering* 9 (4): 311-318.
- Tang XL, Lv X, Li JF (2011) Runoff characteristics of Manasi River Basin in the past 50 years. *Journal of Arid Land Resources and Environment* 25 (5): 124-129. (In Chinese)
- Unger-Shayesteh K, Vorogushyn S, Farinotti D, et al. (2013) What do we know about past changes in the water cycle of Central Asian headwaters? A review. *Global and Planetary Change* 110: 4-25.
- Viessman W, Lewis GL (2002) Introduction to hydrology. Prentice Hall PTR.
- Vogel RM, Kroll CN (1990) Generalized low-flow frequency relationships for ungauged sites in Massachusetts. *Water Resources Bulletin* 26 (2): 241-253.
- Vogel RM, Kroll CN (1992) Regional geohydrologic-geomorphic relationships for the estimation of low-flow statistics. *Water Resources Research* 28 (9): 2451-2458.
- Wang QF, Zhang TJ, Peng XQ (2013) Freezing and thawing processes and their impact on ground surface radiation balance in the upper reaches of Heihe River. *Journal of Lanzhou University (Natural Sciences)* 49 (2): 12-191.
- Wu JC, Sheng Y, Yu H, et al. (2007) Permafrost in the middle-east section of Qilian mountains (I): distribution of permafrost. *Journal of Glaciology and Geocryology* 29: 418-425.
- Xie ZC, Liu CH (2010) An introduction to glaciology. Shanghai Popular Science Press, Shanghai, China.
- Yang ZN (1980) Mountain stream types in northwest China. *Journal of Glaciology and Geocryology* 3: 24-31. (In Chinese)
- Yang ZN (1991) Glacier water resources in China. Gansu Science and Technology Press, Gansu, China. (In Chinese)
- Zhu YH, Day RL (2009) Regression modeling of streamflow, baseflow, and runoff using geographic information systems. *Journal of Environmental Management* 90: 946-953. DOI: 10.1016/j.jenvman.2008.02.011.